

First-principles study of the coverage dependence of the electronic structure of alkali-metal-metal surfaces: Na on Al(001)

H. Ishida and K. Terakura

Institute for Solid State Physics, University of Tokyo, Roppongi, Minato-ku, Tokyo 106, Japan

(Received 6 July 1988)

Coverage (Θ) dependence of the electronic structure of alkali-metal adatoms on a metal surface is studied by a first-principles method, treating both the adatom and substrate [Al(001)] as discrete atoms. The analyses of the charge redistribution, depolarization field, and adatom valence states as well as bond-order and dipole densities as a function of one-electron energy suggest that adatom polarization due to the hybridization of adatom and substrate states plays an important role for Θ dependence of the adatom-induced dipole moment.

In spite of longtime experimental and theoretical efforts, there are a number of unsolved problems with regard to the alkali-metal adsorption on metal surfaces. These include the characteristic variation of the work function with coverage (Θ) and the appearance of overlayer plasmon peaks in the electron-energy-loss spectra.¹⁻⁴ The most important step for understanding them is to clarify the electronic structure of the alkali-metal adatom as a function of Θ . A widely accepted picture proposed first by Gurney⁵ and reinforced later by model calculations based on the Newns-Anderson (NA) Hamiltonian^{6,7} is that the alkali-metal s resonance is located primarily above the Fermi level E_F at low Θ , making the adatom ionic, while the adatom becomes neutral at high Θ due to the depolarization shift of the s resonance. On the other hand, the recent metastable-He deexcitation spectroscopy (MDS) experiment by Woratschek *et al.*⁸ for K/Cu(110) suggests that Θ dependence of the adatom dipole may not be directly associated with the occupation of the s resonance. Soukiassian *et al.*,⁹ and Tochiyama, Kubota, Miyano, and Murata¹⁰ found that the binding energy of the Cs $5p$ core orbital in photoemission spectra is remarkably independent of Θ for Cs/W(001) and Cs/Si(001), respectively. Although there is a possibility that relaxation effects in the final state fortuitously cancel the Θ -dependent chemical shift of Cs $5p$, another naive interpretation may be the invariance of the Cs charge state with respect to Θ . Recently, the present authors reported the first-principles study of the alkali-metal-jellium system¹¹ and showed that the Θ dependence of the charge redistribution around adatoms is quite different from the classical point-charge-transfer picture assumed in the NA model analyses. Furthermore, the bond charge contour which is almost independent of Θ suggests that the charge state of an adatom might be rather insensitive to Θ .

To resolve the above-mentioned controversial subject, we study the electronic structure of the alkali-metal adatom as a function of Θ by a first-principles method, treating both the overlayer and substrate as discrete atoms. The calculation is performed within the local density functional theory combined with the norm-conserving pseudopotential,¹² plane-wave basis, and repeating slab geometry. The substrate in the present work is represented by an unrelaxed five-layer slab of Al(100) with a bulk

lattice constant. We choose Na as alkali-metal.¹³ On the experimental side, the ordered $c(2 \times 2)$ structure ($\Theta = \frac{1}{2}$ in units of Al monolayers) was observed for Na/Al(001).¹⁴⁻¹⁶ Na adatoms sit on a fourfold hollow site, and the perpendicular distance between the Na and top-layer Al atoms was determined as 3.87 a.u. (we use the atomic units where $e = 1$, $m = 1$, and $\hbar = 1$). We calculate the electronic structures of Na/Al(001) for three coverages. The overlayer structure corresponding to the highest Θ is the experimentally observed $c(2 \times 2)$ ($\Theta = \frac{1}{2}$). For lower coverages, we assume $p(2 \times 2)$ ($\Theta = \frac{1}{4}$) and $(\sqrt{8} \times \sqrt{8})R45^\circ$ ($\Theta = \frac{1}{8}$) structures in which Na adatoms sit on the same site as in $\Theta = \frac{1}{2}$ and form a square lattice. The latter two are not experimentally observed but may be meaningful for investigating the distant adatom-adatom interaction. The cutoff energy for plane-wave bases E_{cut} is 6.5 Ry for all the coverages. An additional calculation with $E_{\text{cut}} = 10$ Ry was done for $\Theta = \frac{1}{2}$ to check convergence of the results. The iteration procedure is continued until the difference between the input and output potentials becomes less than 0.1 eV.

First we discuss the charge redistribution due to the interaction between the adatom and substrate. Figure 1 shows the calculated difference charge $\delta\rho(\mathbf{r})$ for three coverages in the vertical-cut plane containing a Na and its nearest two Al atoms. $\delta\rho(\mathbf{r})$ is defined as the charge density of Na/Al(001) minus the superposed density of the isolated Na layer and Al(001) substrate. Apart from the counterpolarization of core orbitals, which is absent in the present pseudopotential calculation, $\delta\rho(\mathbf{r})$ at $\Theta = \frac{1}{2}$ is similar to that of Cs W(001) given by Wimmer, Freeman, Hiskes, and Karo.¹⁷ For lower coverages, kidney-shaped charge depletions appear in the vacuum side of Na and more importantly the buildup of charge density occurs between the neighboring Na and Al atoms irrespective of Θ . These aspects were also seen in the case of jellium substrate.¹¹ The Na induced dipole $d(\Theta)$ at $\Theta = \frac{1}{2}$ is more than three times smaller than that at $\Theta = \frac{1}{8}$. The calculated work functions are 4.6, 3.3, 2.2, and 2.6 eV for $\Theta = 0$, $\frac{1}{8}$, $\frac{1}{4}$, and $\frac{1}{2}$, respectively. It takes a minimum at the $p(2 \times 2)$ coverage ($\Theta = \frac{1}{4}$) as observed for Cs/W(001).¹⁸

In order to study the coverage dependence of the charge

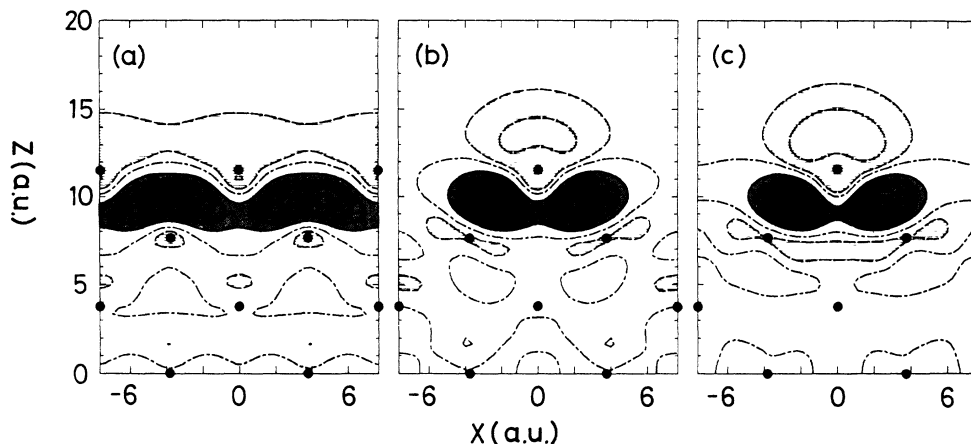


FIG. 1. Contour maps of the difference charge $\delta\rho(\mathbf{r})$ in the vertical-cut plane containing the Na and nearest two Al atoms. (a) $\Theta = \frac{1}{2}$, (b) $\Theta = \frac{1}{4}$, and (c) $\Theta = \frac{1}{8}$. The Na and Al atoms are shown by filled circles. The shaded and hatched areas indicate the regions where $\delta\rho(\mathbf{r}) \geq 0.001$ a.u. and $\delta\rho(\mathbf{r}) \leq -0.0005$ a.u., respectively. The dot-dashed lines correspond to $\delta\rho(\mathbf{r}) = 0$.

state of adatoms, we calculated the adatom induced density of states (DOS) $\rho_a(\varepsilon, \Theta)$ defined by

$$\rho_a(\varepsilon, \Theta) = \int d\mathbf{r} \sum_i |\psi_i^\Theta(\mathbf{r})|^2 \delta(\varepsilon - \varepsilon_i^\Theta) - \int d\mathbf{r} \sum_i |\psi_i^{\Theta=0}(\mathbf{r})|^2 \delta(\varepsilon - \varepsilon_i^{\Theta=0}), \quad (1)$$

where ε_i^Θ and $\psi_i^\Theta(\mathbf{r})$ are the energy and wave function of an electron at coverage Θ , and the integration is done within the sphere of radius R centered at a Na site. The calculated $\rho_a(\varepsilon, \Theta)$ for three coverages are plotted in Fig. 2. The origin of energy is the Fermi level E_F and R is chosen as 3.3 a.u. The dashed curve for $\Theta = \frac{1}{2}$ shows the result calculated with $E_{\text{cut}} = 10$ Ry, which confirms the convergence of the calculation. No significant change in $\rho_a(\varepsilon, \Theta)$ is observed as Θ changes: the spiky-sharp structure at $\Theta = \frac{1}{8}$, which is an artifact caused by our use of a slab geometry, changes to broader one at $\Theta = \frac{1}{2}$ due to the overlap of neighboring Na orbitals, but the important message is that the global peak above E_F at $\Theta = \frac{1}{8}$, which is mainly contributed by $3p$ state, is still above E_F even at $\Theta = \frac{1}{2}$. The number of electrons in a Na atomic sphere $n_a(\Theta)$ obtained by integrating $\rho_a(\varepsilon, \Theta)$ up to E_F changes only by ~ 0.05 electrons as one goes from $\Theta = \frac{1}{8}$ to $\frac{1}{2}$: $n_a^{\frac{1}{8}} = 0.39$ and $n_a^{\frac{1}{2}} = 0.44$. Moreover, $n_a(\Theta)$ is ~ 0.03 electrons larger than the number of electrons within the same sphere calculated for the corresponding isolated Na monolayer [$n_a^{\text{iso}}(\Theta)$] regardless of Θ , which suggests that the adatom region is essentially neutral even at low Θ .

The insensitivity of $\rho_a(\varepsilon, \Theta)$ and $n_a(\Theta)$ to Θ is in accord with the recent experiments.⁸⁻¹⁰ However, the above argument alone may not be decisive because of the ambiguity inherent to the definition of the charge state. A more fundamental quantity is the depolarization field at the adatom site, which can be estimated as the electrostatic potential $\delta\phi_{\text{el}}(\mathbf{r})$ associated with $\delta\rho(\mathbf{r})$. Simplified models based on the NA Hamiltonian^{6,7} predict its lowering in an order of 1 eV with increasing Θ , which is indispensable to a drastic change in the adatom charge state. Figure 3 shows $\delta\phi_{\text{el}}(\mathbf{r})$ along a vertical axis containing a Na.

$\delta\phi_{\text{el}}(\mathbf{r})$ as measured from the interior of Al(001) is lowered in the vacuum side of a Na due to the adatom dipole fields, which thus results in the work function lowering. Furthermore, $\delta\phi_{\text{el}}(z = \infty)$ varies significantly with Θ . On the other hand, $\delta\phi_{\text{el}}(\mathbf{r})$ exhibits no appreciable variation with Θ at Na sites. In the same way, the calculated s part of the total potential including the exchange-correlation part within a Na atomic sphere hardly depends on Θ . This is consistent with the insensitivity of $n_a(\Theta)$ to Θ and implies an efficient screening effect near the surface of Al(001) and concomitantly the short-range character of $\delta\phi_{\text{el}}(\mathbf{r})$ in the adatom plane.

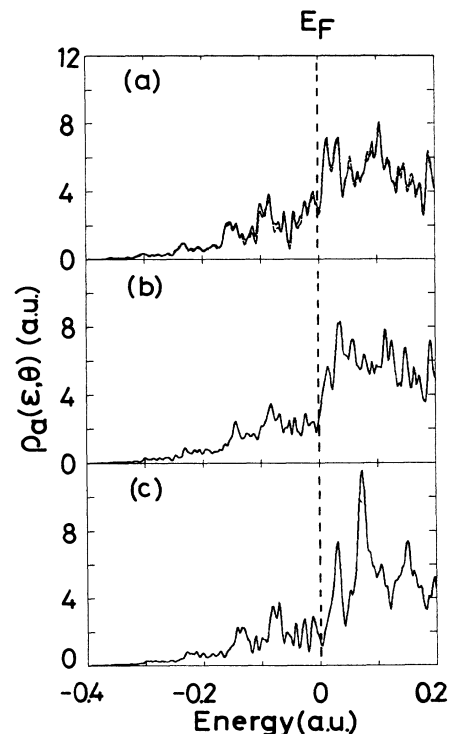


FIG. 2. The calculated $\rho_a(\varepsilon, \Theta)$ for (a) $\Theta = \frac{1}{2}$, (b) $\Theta = \frac{1}{4}$, and (c) $\Theta = \frac{1}{8}$. The units of the energy is 27.2 eV.

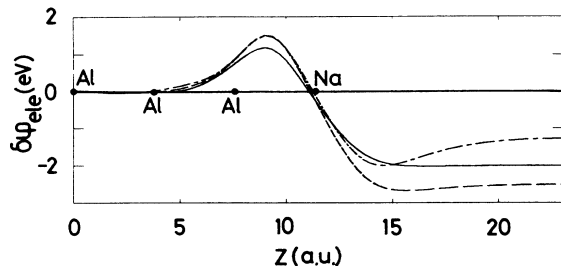


FIG. 3. $\delta\phi_{\text{ele}}(r)$ along a vertical axis containing a Na atom. The solid, dashed, and dot-dashed lines correspond to $\Theta = \frac{1}{2}$, $\frac{1}{4}$, and $\frac{1}{8}$, respectively.

How can we explain a rapid decrease of $d(\Theta)$ with increasing Θ if the adatom charge state is rather insensitive to Θ . In the model analyses based on the NA model, one assumes that $d(\Theta)$ is in proportion to the charge transfer. However, $d(\Theta)$ should additionally include a polarization term arising from the hybridization of adatom and substrate orbitals, and should be written as

$$d(\Theta) = D(1 - \langle C_a^\dagger C_a \rangle) + \sum_{ab} \mu_{ab} \langle C_a^\dagger C_b \rangle + \text{c.c.}, \quad (2)$$

where a and b denote the adatom and substrate states, and D and μ_{ab} are dipole matrix elements.¹⁹ The origin of the second term is the inward (outward) polarization of the electron wave functions characteristic to the adatom-substrate bonding (antibonding) states. The charge-transfer-induced dipole disappears when an adatom is neutral, while the polarization-induced one becomes the largest when E_F is at the bonding-antibonding (B-A) boundary, which is usually near the resonant center.

To elucidate the nature of the adatom-substrate bonding in the present system, we calculate the bond-order density $\beta(\epsilon, \Theta)$ defined by $\sum_i \text{Re} \psi_i^\Theta(\mathbf{r}_1) \psi_i^{\Theta*}(\mathbf{r}_2) \delta(\epsilon - \epsilon_i^\Theta)$ where \mathbf{r}_1 and \mathbf{r}_2 are taken at Na and nearest Al sites. The calculated $\beta(\epsilon, \Theta)$ are shown in Fig. 4 by solid lines. The positive and negative parts correspond to the bonding and antibonding states, respectively. The B-A boundary coincides almost perfectly with E_F at $\Theta = \frac{1}{8}$, which indicates an importance of the adatom polarization to $d(\Theta)$ as well as a formation of a metallic adatom-substrate bond by the maximum use of bonding states even at low Θ . To support the above argument, we further calculate the dipole density defined as

$$\mu(\epsilon, \Theta) = \int d\mathbf{r} \sum_i \psi_{i,s}^\Theta(\mathbf{r}) \psi_{i,p_z}^{\Theta*}(\mathbf{r}) z \delta(\epsilon - \epsilon_i^\Theta), \quad (3)$$

where $\psi_{i,s}^\Theta(\mathbf{r})$ and $\psi_{i,p_z}^\Theta(\mathbf{r})$ are s and p_z components of $\psi_i^\Theta(\mathbf{r})$ within a Na atomic sphere, and the integration region is the same as for $\rho_a(\epsilon, \Theta)$. Our partial density-of-states analysis of a Na atom revealed that Na $3p_z$ is essentially located above E_F ; thus Eq. (3) may be interpreted as giving a dipole caused by the mixing of the Na $3s$ and p_z part of the substrate states rather than the intra-atomic polarization (Na $3s$ - $3p_z$ mixing). The calculated $\mu(\epsilon, \Theta)$ is shown in Fig. 4 by dashed lines, where its positive sign corresponds to the inward polarization of electron wave functions which lowers the work function. The close similarity between $\beta(\epsilon, \Theta)$ and $\mu(\epsilon, \Theta)$ as well as its characteristic energy dependence reconfirms the important role

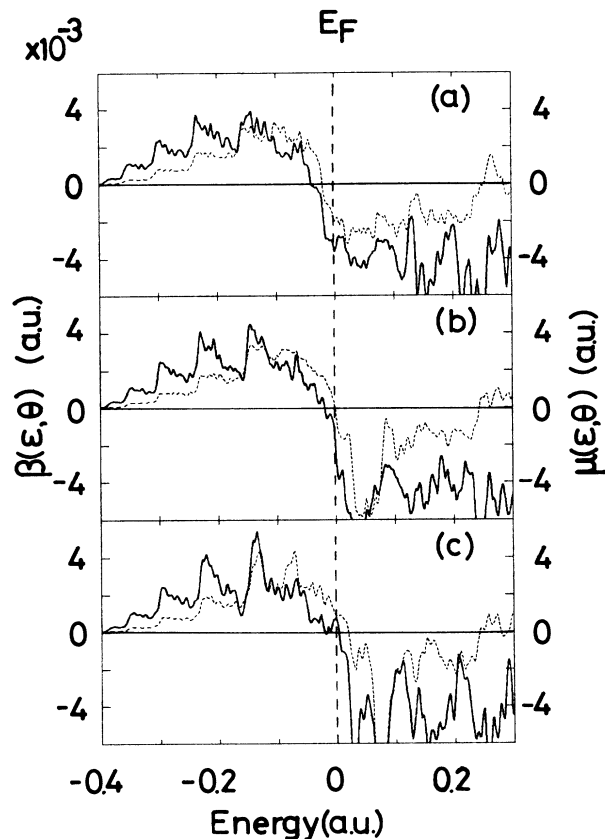


FIG. 4. The calculated $\beta(\epsilon, \Theta)$ (solid lines) and $\mu(\epsilon, \Theta)$ (dashed lines) for (a) $\Theta = \frac{1}{2}$, (b) $\Theta = \frac{1}{4}$, and (c) $\Theta = \frac{1}{8}$.

of the off-diagonal polarization effect to $d(\Theta)$.

With the second term of Eq. (2), the rapid decrease of $d(\Theta)$ with increasing Θ is naturally explained as follows. One is the weakening in the substrate-adatom bonding ($\propto \langle C_a^\dagger C_b \rangle$) which follows the strengthening in the adatom-adatom interaction with increasing Θ . Such a bond weakening has been observed in many experiments as a decrease in the desorption energy of adatoms with increasing Θ , and is the origin of the commensurate-incommensurate transition of the overlayer structure.²⁰ In the present calculation, the calculated binding energies of a Na are 2.9, 2.5, and 2.2 eV for $\Theta = \frac{1}{8}$, $\frac{1}{4}$, and $\frac{1}{2}$, respectively. Secondly, the dipole matrix element μ_{ab} should become significantly smaller with increasing Θ . This effect is seen in Fig. 1 as an inward shift of the charge depletion region on the Na side. The effective dipole length at $\Theta = \frac{1}{2}$ is estimated as $\sim 60\%$ of that at $\Theta = \frac{1}{8}$.

In conclusion, we studied Θ dependence of the electronic structure of the alkali-metal adatom on a metal surface by a first-principles method, treating both the adatom and substrate as discrete atoms. We suggested that Θ dependence of the adatom charge state may be considerably smaller than that evaluated by simplified models based on the NA Hamiltonian. We emphasized that even in such cases the rapid decrease of $d(\Theta)$ with increasing Θ can be well understood in terms of the Θ -dependent adatom polarization.

This work is partially supported by a Grant-in-Aid for Scientific Research on Priority Areas by the Ministry of the Education, Science, and Culture. The numerical computation was done at the Computer Centers of University of Tokyo, Institute for Molecular Science and Institute for Solid State Physics.

-
- ¹J. P. Muscat and D. M. Newns, *Prog. Surf. Sci.* **9**, 1 (1978).
²T. Aruga, H. Tochiara, and Y. Murata, *Phys. Rev. B* **34**, 8237 (1986).
³A. Hohlfeld, M. Sunjic, and K. Horn, *J. Vac. Sci. Technol. A* **5**, 679 (1987).
⁴H. Ishida and M. Tsukada, *Surf. Sci.* **169**, 225 (1986).
⁵R. W. Gurney, *Phys. Rev.* **47**, 479 (1935).
⁶J. P. Muscat and D. M. Newns, *J. Phys. C* **7**, 2630 (1974).
⁷J. P. Muscat and I. P. Batra, *Phys. Rev. B* **34**, 2889 (1986).
⁸B. Woratschek, W. Sesselmann, J. Küppers, G. Ertl, and H. Haberland, *Phys. Rev. Lett.* **55**, 1231 (1985).
⁹P. Soukiassian, R. Riwan, J. Lecante, E. Wimmer, S. R. Chubb, and A. J. Freeman, *Phys. Rev. B* **31**, 4911 (1985).
¹⁰H. Tochiara, M. Kubota, M. Miyano, and Y. Murata, *Surf. Sci.* **158**, 497 (1985).
¹¹H. Ishida and K. Terakura, *Phys. Rev. B* **36**, 4510 (1987).
¹²G. B. Bachelet, D. R. Hamann, and M. Schluter, *Phys. Rev. B* **26**, 4199 (1982).
¹³Na adatoms are adsorbed on both sides of the substrate to retain symmetry. The vacuum region between neighboring slabs has a thickness of 23 a.u. which is wide enough for evaluating the work function.
¹⁴J. O. Porteus, *Surf. Sci.* **41**, 515 (1974).
¹⁵M. Van Hove, S. Y. Tong, and N. Stoner, *Surf. Sci.* **54**, 259 (1976).
¹⁶B. A. Hutchins, T. N. Rhodin, and J. E. Demuth, *Surf. Sci.* **54**, 419 (1976).
¹⁷E. Wimmer, A. J. Freeman, J. R. Hiskes, and A. R. Karo, *Phys. Rev. B* **28**, 3074 (1983).
¹⁸C. A. Papageorgopoulos and J. M. Chen, *Surf. Sci.* **39**, 283 (1973).
¹⁹H. Ishida, *Phys. Rev. B* (to be published).
²⁰T. Aruga, H. Tochiara, and Y. Murata, *Surf. Sci.* **158**, 490 (1985).

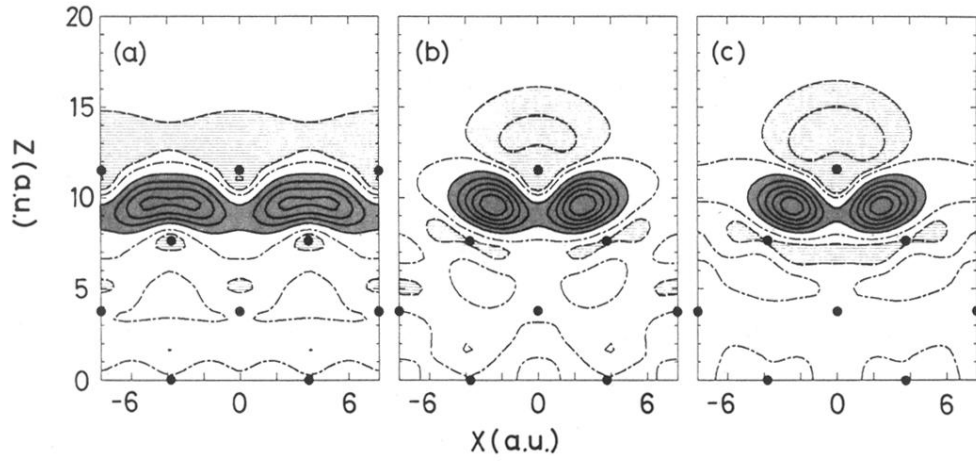


FIG. 1. Contour maps of the difference charge $\delta\rho(\mathbf{r})$ in the vertical-cut plane containing the Na and nearest two Al atoms. (a) $\Theta = \frac{1}{2}$, (b) $\Theta = \frac{1}{4}$, and (c) $\Theta = \frac{1}{8}$. The Na and Al atoms are shown by filled circles. The shaded and hatched areas indicate the regions where $\delta\rho(\mathbf{r}) \geq 0.001$ a.u. and $\delta\rho(\mathbf{r}) \leq -0.0005$ a.u., respectively. The dot-dashed lines correspond to $\delta\rho(\mathbf{r}) = 0$.